DOI: 10.26599/FSHW.2026.9251114

Contents lists available at SciOpen

Food Science and Human Wellness

journal homepage: https://www.sciopen.com/journal/2097-0765

China Food Publishing Co.

Bifidobacterium breve B2798 ameliorates high-fat diet-induced obesity by reshaping gut microbiota and modulating host metabolic profiles

Yue Zhao[1], Lai-Yu Kwok[1], Guangqi Gao[1], Na Li[1], Chunyan Zhao[1], Zhihong Sun[1]*, Jie Yu[1]*

[1] *Inner Mongolia Key Laboratory of Dairy Biotechnology and Engineering, Key Laboratory of Dairy Products Processing, Ministry of Agriculture and Rural Affairs, Key Laboratory of Dairy Biotechnology and Engineering, Ministry of Education, Inner Mongolia Agricultural University, National Collection of Microbial Resource for Feed (Inner Mongolia), Hohhot, Inner Mongolia 010018, China*

ABSTRACT: Obesity is a global health challenge closely linked to gut microbiota dysbiosis. This study investigated the anti-obesity effects of *Bifidobacterium breve* B2798 in a high-fat diet (HFD)-induced mouse model. Male C57BL/6 mice were fed a 60% HFD with or without daily oral administration of *B. breve* B2798 12 weeks. Probiotic intervention significantly reduced body weight gain, visceral adiposity, and hepatic steatosis compared to the HFD group. Serum lipid profiling revealed increased HDL-C levels in the probiotic-treated group, indicating improved metabolic health. Fecal metagenomic analysis showed that *B. breve* B2798 reshaped the gut microbiota, enriching beneficial taxa such as *Ligilactobacillus* while reducing pro-inflammatory *Faecalibaculum rodentium*. Untargeted metabolomics of fecal and serum samples revealed significant modulation of metabolic pathways, including bile acid metabolism, amino acid biosynthesis, and short-chain fatty acid production. Key metabolites such as chenodeoxycholic acid, limonin, azelaic acid, and syringic acid were elevated in the *B. breve* B2798-treated group and are linked to anti-obesity and anti-inflammatory effects. Integrated correlation analysis demonstrated strong associations between microbial shifts, metabolic changes, and improved phenotypes. These findings, obtained in a murine model, suggest that *B. breve* B2798 alleviates obesity through a gut microbiota-host metabolic axis, offering a promising adjunctive probiotic strategy for metabolic disease prevention.

Keywords: Gut microbiome, Metabolomics, Dysbiosis, Probiotic intervention, Bile acids, Adipose tissue, Metabolic syndrome

1. Introduction

Obesity is a chronic and multifactorial disease characterized by excessive adipose tissue accumulation, leading to a heightened risk of type 2 diabetes, cardiovascular diseases, musculoskeletal disorders, reproductive dysfunction, and certain cancers. It also impairs quality of life through disrupted sleep, reduced physical mobility, and psychological distress. Globally, obesity has reached epidemic proportions. This shifting burden is particularly striking among children and adolescents. According to the United Nations Children's Fund (UNICEF), between 2000 and 2024, the global prevalence of underweight among children and adolescents aged 5–19 years declined from nearly 13% to 9.2%. Over the same period, however, the

***Corresponding author**
yujie8301@sina.com, sunzhihong78@163.com

Received 22 December 2025
Received in revised from 13 February 2026
Accepted 30 March 2026

prevalence of obesity more than tripled, rising from 3% to 9.4% . For the first time, in all global regions except sub-Saharan Africa and South Asia, the prevalence of obesity has surpassed that of underweight, marking a fundamental transition in the pattern of childhood malnutrition [1]. These alarming trends highlight the urgent need for effective prevention and intervention strategies.

At its core, obesity arises from a sustained positive energy balance, when caloric intake exceeds expenditure; this imbalance is influenced by genetic, behavioral, psychological, and environmental factors. Mounting evidence implicates the gut microbiota as a key regulator of host energy homeostasis and metabolic health. Dysbiosis, or disruption of the microbial ecosystem, is frequently observed in obesity and is associated with increased energy harvest, impaired gut barrier function, systemic inflammation, and metabolic endotoxemia[2]. A hallmark of obesity-related dysbiosis is an elevated Firmicutes-to-Bacteroidetes ratio[3]. Moreover, a growing body of evidence demonstrates that gut microbes influence host energy balance by modulating the extraction and storage of nutrients from the diet[5]. Seminal work by Bäckhed et al. (2004) showed that transferring cecal microbiota from conventional mice into germ-free mice resulted in a 60% increase in epididymal fat mass and the development of insulin resistance, despite no change in food intake[4]. This landmark finding provided direct experimental evidence that the gut microbiota actively contributes to host adiposity and metabolic dysfunction, reinforcing the concept that microbial communities are not merely bystanders but active regulators of energy metabolism. The gut microbiota also plays a vital role in nutrient metabolism, immune modulation, and pathogen defense[5]. However, factors such as high-fat diets, antibiotics, and chronic stress can destabilize this ecosystem, contributing to metabolic disease[6].Given this critical role, targeting the gut microbiota has emerged as a promising therapeutic avenue for obesity management.

Probiotics, defined as “live microorganisms which, when administered in adequate amounts, confer a health benefit on the host”[7], have gained attention for their potential to restore microbial balance and improve metabolic outcomes. Probiotic supplementation may mitigate obesity by enhancing gut barrier integrity, reducing low-grade inflammation, modulating immune responses, and influencing host signaling pathways related to appetite and metabolism[8].

Preclinical and clinical studies have demonstrated that specific probiotic strains can exert anti-obesity effects. For instance, a previous study reported that VSL#3, a high-potency multi-strain probiotic, not only suppressed weight gain but also improved insulin sensitivity in animal models. These benefits were associated with a restructuring of the gut microbiota and increased secretion of glucagon-like peptide-1, an enteroendocrine hormone that enhances satiety, reduces food intake, and improves glucose homeostasis[9].

Further support comes from a comprehensive meta-analysis conducted by Ejtahed et al. (2020), investigating the impact of probiotics on obesity[10]. The study found that certain lactobacilli and bifidobacteria strains effectively ameliorated obesity. Importantly, the anti-obesity effects were highly strain-specific, underscoring the importance of precise microbial selection in probiotic interventions[10]. Together, these findings highlight the therapeutic potential of probiotics in modulating the gut microbiota to combat obesity, while also emphasizing the need for targeted, evidence-based approaches in their application.

Bifidobacterium breve B2798, isolated from the feces of infant in Enshi, Hubei province, is currently stored at the Lactobacillus Culture Center of the Key Laboratory of Dairy Biotechnology and Engineering at Inner Mongolia Agricultural University. This strain exhibits characteristics of acid and bile salt resistance, along with anti-inflammatory and antibacterial properties[11].Here, we investigate the effects of *Bifidobacterium breve* B2798 (*B. breve* B2798) in a high-fat diet (HFD)-induced obesity model in C57BL/6 mice. Using a combination of physiological, biochemical, histopathological, metagenomic, and untargeted metabolomic approaches, we demonstrate that *B. breve* B2798 supplementation attenuates weight gain, remodels the gut microbiota, and reprograms fecal and serum metabolic profiles, revealing a gut microbiome-host metabolic axis underlying its protective effects.

2. Results

2.1 Bifidobacterium breve B2798 Attenuates Diet-Induced Obesity and Improves Metabolic Tissue Pathology

To evaluate the anti-obesity potential of *B. breve* B2798, this study established a diet-induced obesity model in male C57BL/6 mice using a 60% HFD diet for 12 weeks, with concurrent daily oral administration of the probiotic (2×10^9 CFU/mouse/day, resuspended in saline) (Figure 1A).Mice were randomly classified into three groups (n = 8 per group): normal chow (NC), high-fat diet (HFD), or HFD supplemented with *B. breve* B2798 (BB).

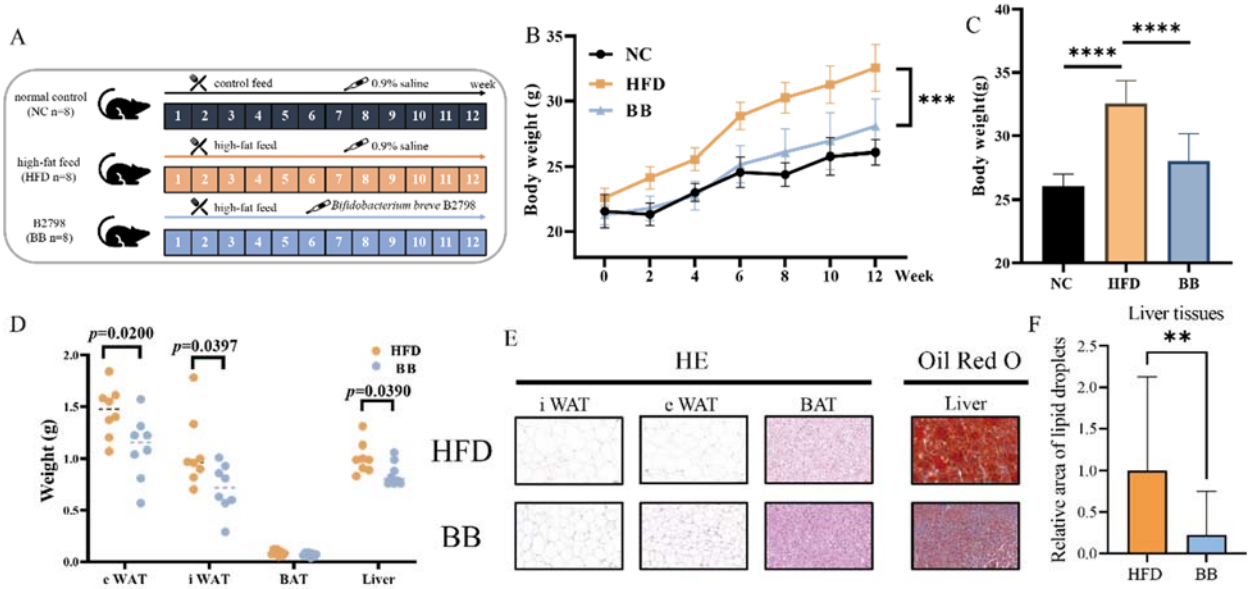

Figure 1. *Bifidobacterium breve* B2798 attenuates high-fat diet-induced obesity and ameliorates adipose-liver axis pathology in mice. (A) Experimental design schematic. Six-week-old male C57BL/6 mice were acclimated for one week and then randomly assigned to three groups (n = 8 per group): normal chow (NC), high-fat diet (HFD), or HFD supplemented with *B. breve* B2798 (BB). Oral gavage was administered daily for 12 weeks. (B) Biweekly body weight changes throughout the intervention period. (C) Final body weights at week 12. (D) Absolute weights of epididymal white adipose tissue (eWAT), inguinal white adipose tissue (iWAT), brown adipose tissue (BAT), and liver at euthanasia. (E) Representative histological sections of eWAT, iWAT, and BAT were stained with hematoxylin and eosin (H&E); liver sections were stained with oil red O to visualize lipid accumulation (scale bars, 100 μm).(F) Quantitative analysis of Oil Red O staining in liver sections. The relative lipid droplet area was quantified using ImageJ and normalized to the HFD group (set as 100%). Data are presented as mean ± SD (n = 8 per group). Error bars represent the standard deviation. Statistical differences were evaluated using the one-way ANOVA or Mann-Whitney test, with $P < 0.05$ considered statistically significant (** $P < 0.01$, *** $P < 0.001$, **** $P < 0.0001$).

Body weight was monitored throughout the 12-week intervention period. Mice in the BB group exhibited a significantly lower weight gain rate compared to the HFD control group (Figure 1B). By the end of the study, the BB group had markedly lower final body weights than the HFD group and showed no significant difference from the NC group ($P < 0.001$ vs. HFD group, $P > 0.05$ vs. NC group; Figure 1C), indicating that *B. breve* B2798 effectively attenuated HFD-induced body weight gain.

At sacrifice, key metabolic tissues were dissected and weighed. Compared to the HFD group, the BB group showed significant reductions in the mass of epididymal white adipose tissue (eWAT, $p = 0.02$), inguinal white adipose tissue (iWAT, $p = 0.0397$), and liver ($p = 0.039$), while brown adipose tissue (BAT) mass did not differ significantly between groups (Figure 1D). These findings suggest that *B. breve* B2798 supplementation specifically counteracts excessive lipid storage in white adipose depots and reduces liver weight.

Histological analysis further confirmed these observations (Figure 1E). Hematoxylin and eosin staining of iWAT and eWAT from HFD-fed mice revealed pronounced adipocyte hypertrophy, characterized by large, unilocular lipid droplets and compressed nuclei, classic features of obesity-induced adipose expansion. In contrast, adipocytes in the BB group were noticeably smaller and more uniformly sized, indicating reduced lipid storage and improved adipose tissue health. BAT from HFD mice displayed disrupted multilocular architecture, with enlarged and fused lipid vacuoles, consistent with impaired thermogenic activity. Notably, BAT in the BB group preserved a more typical multilocular morphology, suggesting partial preservation or restoration of thermogenic function. Liver sections from the HFD group showed extensive lipid accumulation, as revealed by Oil Red O staining, with large, confluent red-stained lipid droplets throughout the parenchyma, hallmarks of severe hepatic steatosis. Quantitative analysis of the relative lipid droplet area confirmed that the BB group exhibited a significant reduction compared to the HFD group ($P < 0.01$; Figure 1F) In contrast, the BB group exhibited a dramatic reduction in lipid deposition, with fewer and smaller lipid droplets, indicating that *B. breve* B2798 ameliorates diet-induced fatty liver. Collectively, these results demonstrate that *B. breve* B2798 supplementation effectively mitigates high-fat diet-induced obesity, reduces adiposity, protects against hepatic steatosis, and helps preserve the structural and functional integrity of both white and brown adipose tissues.

2.2 Bifidobacterium breve B2798 Modulates Serum Lipid Metabolism in High-Fat Diet-Fed Mice

To evaluate the systemic metabolic impact of *B. breve* B2798 supplementation, serum lipid profiles were analyzed in mice from the NC, HFD, and BB groups (Figures 2). Surprisingly, mice in the HFD group exhibited significantly lower total cholesterol (TC) levels compared to the NC group ($P < 0.05$), while the BB group showed a significant increase in TC relative to the HFD group ($P < 0.05$). This rise in TC in the BB group was primarily driven by a notable increase in high-density lipoprotein cholesterol (HDL-C), which was significantly elevated compared to the HFD group ($P < 0.01$). Higher HDL-C levels are generally associated with improved reverse cholesterol transport and reduced cardiovascular risk, suggesting a beneficial shift in lipid metabolism upon probiotic intervention.

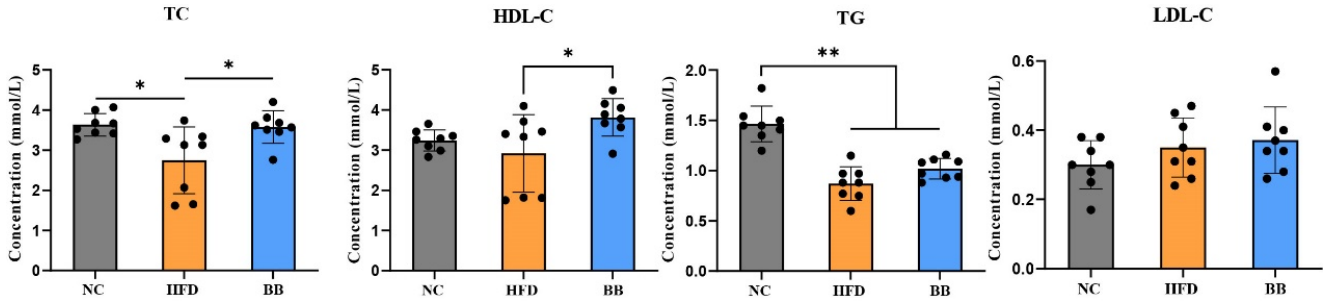

Figure 2. *Bifidobacterium breve* B2798 modulates systemic lipid metabolism, increasing HDL-C in high-fat diet-fed mice. Serum lipid profiles were analyzed in mice from three experimental groups (n = 8 per group): normal chow (NC), high-fat diet (HFD), and HFD supplemented with *B. breve* B2798 (BB) post-intervention. The measured parameters included total cholesterol (TC), triglycerides (TG), high-density lipoprotein cholesterol (HDL-C), and low-density lipoprotein cholesterol (LDL-C). Error bars represented the standard deviation. Statistical differences were evaluated using the one-way ANOVA, with $P < 0.05$ considered statistically significant (* $P < 0.05$, ** $P < 0.01$).

Triglyceride (TG) levels were markedly reduced in the HFD group compared to the NC group ($P < 0.01$), a finding that may reflect metabolic dysregulation or altered hepatic lipid handling under prolonged high-fat feeding. Importantly, the BB group displayed a moderate but detectable increase in TG levels relative to the HFD group, trending toward normalization, although the difference did not reach statistical significance compared to the NC group.

In contrast, no significant differences were observed in low-density lipoprotein cholesterol (LDL-C) levels among the three groups, indicating that probiotic supplementation did not substantially alter this atherogenic lipoprotein fraction under the experimental conditions.

These results suggest that while HFD feeding disrupts normal lipid homeostasis, supplementation with *B. breve* B2798 induces a favorable redistribution of circulating lipids, particularly by elevating HDL-C, pointing to a potential role for this probiotic strain in promoting a more cardioprotective lipid profile despite ongoing high-fat dietary challenge.

2.3 Bifidobacterium breve B2798 Remodels Gut Microbial Composition in High-Fat Diet-Fed Mice

To assess the impact of *B. breve* B2798 on the gut microbiota, metagenomic sequencing was performed on the fecal samples from the NC, HFD, and BB groups. Alpha diversity analysis, based on the Shannon and Simpson indices, revealed that the HFD significantly increased microbial diversity compared to the NC group ($P < 0.001$),indicating a state of diet-induced dysbiosis characterized by altered community structure . However, probiotic intervention did not restore alpha diversity to NC levels, suggesting that the probiotic did not broadly rescue overall microbial richness or evenness in this context (Figure 3A).

In contrast, beta diversity analysis based on Bray–Curtis dissimilarity revealed a clear separation in microbial community structure among the three groups ($R = 0.755 – 0.983$, $p = 0.001$, analysis of similarity test; Figure 3B). Notably, the BB group formed a distinct cluster, spatially separated from both the NC and HFD groups, indicating that *B. breve* B2798 induced a unique and substantial shift in the overall gut microbiome architecture, independent of diet-induced dysbiosis.

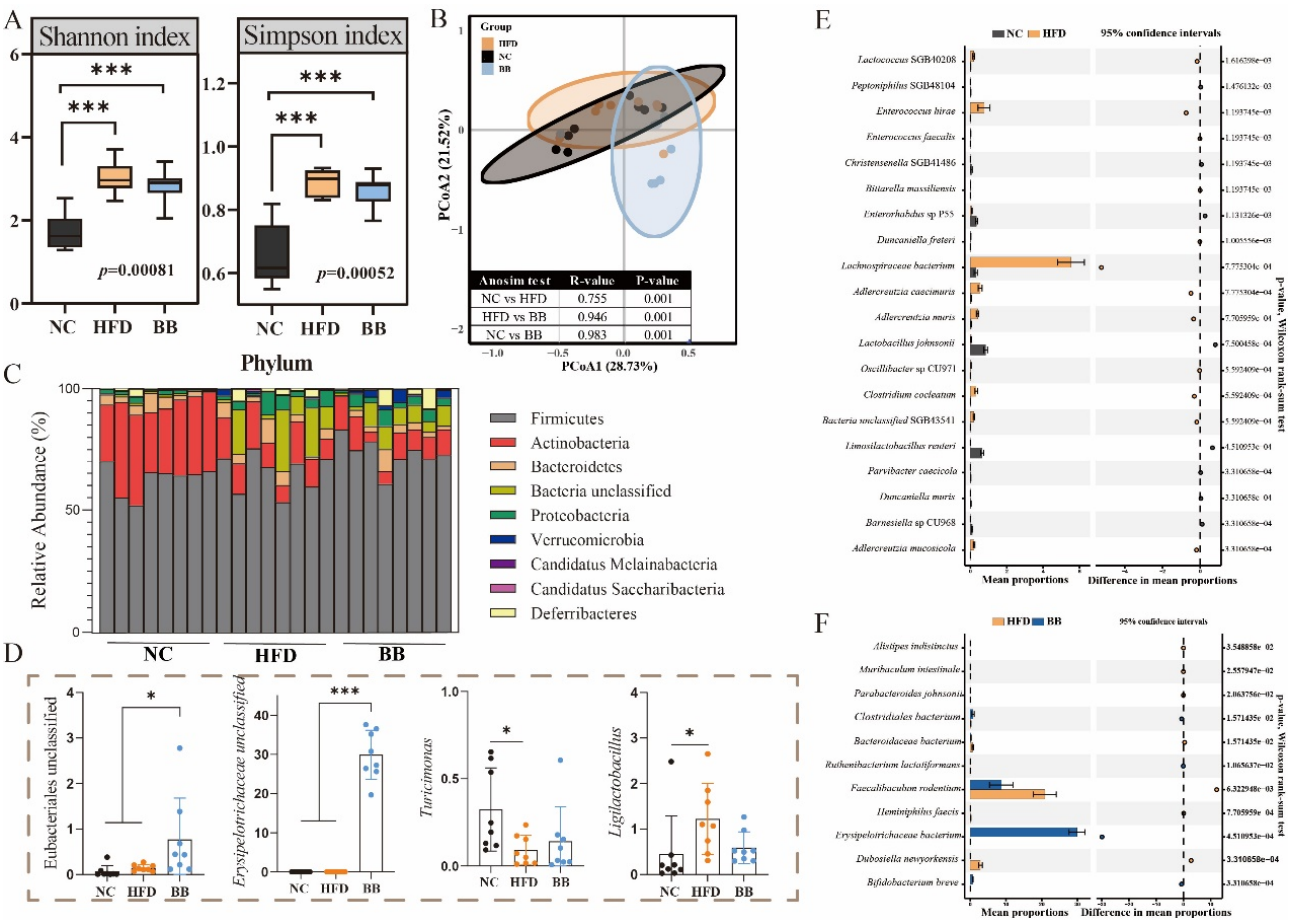

Figure 3. *Bifidobacterium breve* B2798 reshapes gut microbiota composition and partially restores taxon-specific balance in high-fat diet-induced dysbiosis. Fecal samples from the normal chow (NC), high-fat diet (HFD), and HFD supplemented with *B. breve* B2798-treated (BB) groups (n = 8 per group) were analyzed via metagenomic sequencing. (A) Alpha diversity was assessed using Shannon and Simpson diversity indices. (B) Beta diversity analysis of the fecal metagenomes of the three groups via principal coordinates analysis (PCoA; Bray-Curtis distances) and analysis of similarity (ANOSIM). (C) Phylum-level taxonomic composition showing shifts in relative abundances of major phyla. (D) Genus-level profiles highlighting significant changes; statistical comparisons were performed using the Wilcoxon rank-sum test, with $P < 0.05$ considered significance (* $P < 0.05$, *** $P < 0.001$). (E, F) STAMP analysis identified differentially abundant species between (E) NC vs. HFD and (F) HFD vs. BB groups (cut-off level: $P < 0.05$). Error bars represent the standard deviation.

At the phylum level, the BB group exhibited decreased relative abundances of Actinobacteria, Bacteroidetes, and Proteobacteria compared to the HFD group (Figure 3C), reflecting a major reorganization of dominant microbial lineages. At the genus level, the BB group showed significant increases in Eubacteriales unclassified ($P < 0.05$) and *Erysipelotrichaceae* unclassified ($P < 0.001$), taxa associated with improved metabolic health in some contexts.

STAMP-based comparative analysis at the species level further revealed distinct microbial shifts (Figures 3E and 3F). Relative to the NC group, the HFD group exhibited elevated levels of *Enterococcus hirae*, *Lachnospiraceae bacterium*, and *Adlercreutzia caecimuris*, along with reduced abundances of beneficial species such as *Enterorhabdus* sp. P55, *Lactobacillus johnsonii*, and *Limosilactobacillus reuteri* ($P < 0.05$ in all cases), consistent with diet-induced dysbiosis. In comparison to the HFD group, the BB group showed significant enrichment of *B. breve*, *Ruthenibacterium lactatiformans*, and *Erysipelotrichaceae bacterium* ($P < 0.05$), while exhibiting marked reductions in *Faecalibaculum rodentium* and *Bacteroidaceae bacterium* ($P < 0.05$).

These findings demonstrate that although *B. breve* B2798 did not restore overall microbial diversity, it profoundly reshaped the gut microbiota, promoting the expansion of beneficial or health-associated taxa and suppressing potentially detrimental species. This targeted remodeling of the microbial community may underlie the observed metabolic improvements in the BB group.

2.4 Bifidobacterium breve B2798 Alters the Fecal Metabolomic Profile and Modulates Key Metabolic Pathways in High-Fat Diet-Fed Mice

To explore the functional consequences of *B. breve* B2798 supplementation on host-microbiota metabolic interactions, untargeted metabolomic analysis was performed on fecal samples from the three groups. Principal component analysis revealed clear separation between the NC group and those received HFD in both positive and negative ion modes (Figure 4A), indicating profound metabolic shifts induced by high-fat feeding. Further partial least squares discriminant analysis further revealed well-defined clustering among all three groups and demonstrated high model validity ($R^2 = 0.95$, $Q^2 = 0.77$; Figure 4B), confirming the reliability of the metabolic discrimination (Figure 4B).

Dot plot analysis identified a large number of differentially abundant metabolites across pairwise comparisons (Figure 4C). In the NC vs HFD group comparison, 275 metabolites increased significantly and 445 decreased, reflecting widespread metabolic disruption due to HFD. In contrast, the HFD group vs BB group comparison revealed 32 increased and 136 decreased metabolites, indicating that the probiotic intervention induces a more targeted but functionally significant metabolic shift.

An UpSet plot illustrated that 107 differential metabolites were unique to the NC group vs HFD group comparison, while 61 metabolites were unique to the HFD group vs BB group comparison, highlighting both diet- and probiotic-specific metabolic signatures (Figure 4D). Among the metabolites altered by *B. breve* B2798, five were selected for in-depth examination due to their biological relevance: piericidinC1, isodeoxycholic acid , tacrolimus, limonin , and chenodeoxycholic acid. All five were significantly elevated in the BB group compared to both the HFD and NC groups ($P < 0.05$; Figure 4E).

Kyoto Encyclopedia of Genes and Genomes (KEGG) pathway enrichment analysis of the differentially abundant metabolites between the HFD and BB groups identified the top 20 significantly enriched pathways, with seven directly linked to the metabolism category. Of particular interest were 2-oxocarboxylic acid metabolism, biosynthesis of amino acids, and pantothenate and CoA biosynthesis, all central to energy production, microbial fermentation, and coenzyme synthesis (Figure 4F). These pathways are closely tied to microbial metabolic activity and host energy regulation, implying that *B. breve* B2798 may exert its beneficial effects by restoring metabolic flux in key microbial and host-related biochemical networks.

Collectively, these results demonstrate that *B. breve* B2798 not only counteracts HFD-induced metabolic dysregulation in the gut but also promotes the accumulation of bioactive metabolites and reactivates critical metabolic pathways, potentially contributing to improved systemic metabolic health.

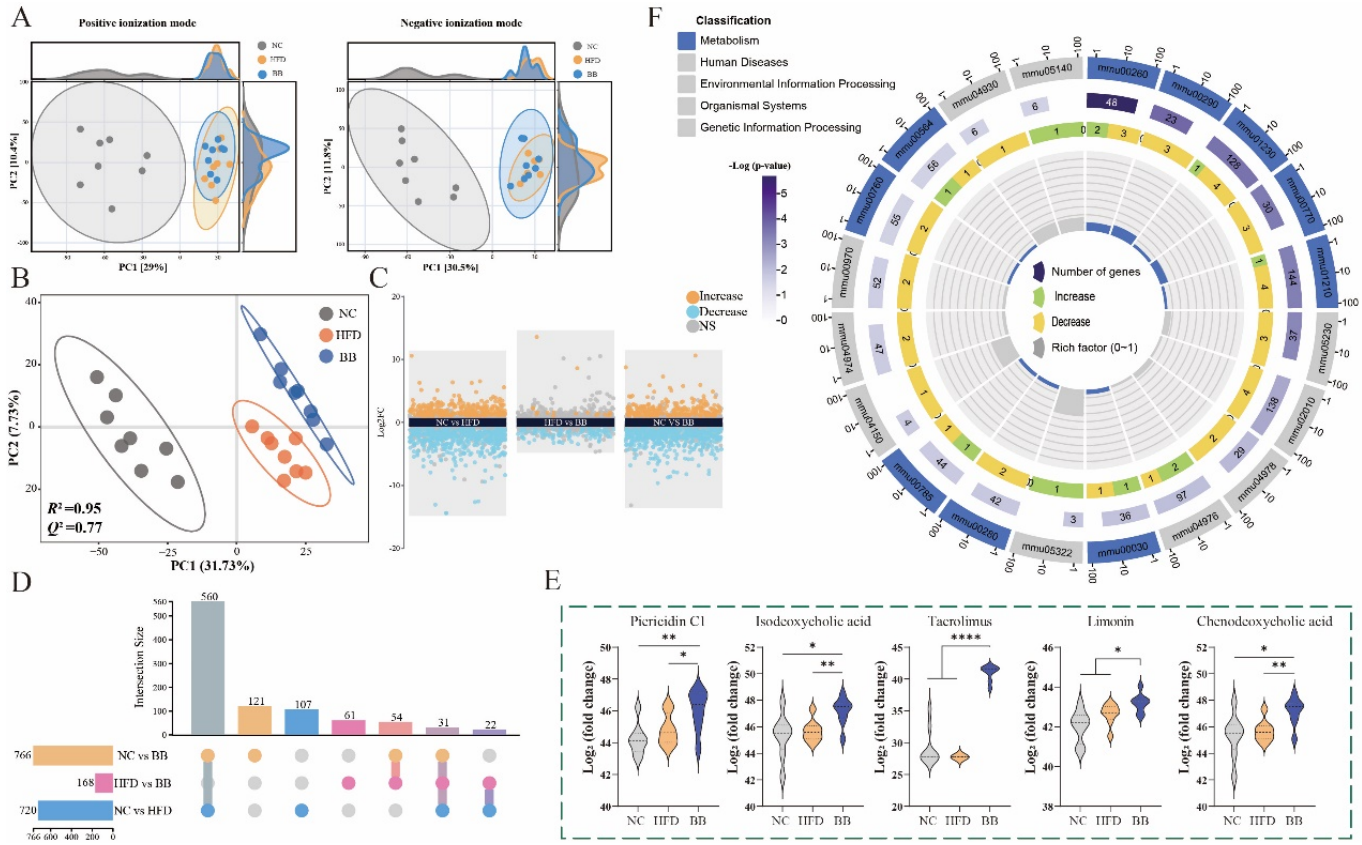

Figure 4. Fecal metabolomic profiling reveals *Bifidobacterium breve* B2798-driven reprogramming of gut metabolic functions in high-fat diet-fed mice. Untargeted metabolomic analysis was performed on fecal samples from the normal chow (NC), high-fat diet (HFD), and HFD supplemented with *B. breve* B2798 (BB) groups (n = 8 per group). (A) Principal Component Analysis (PCA) plots show clear separation of metabolic profiles in both positive and negative ionization modes, with distinct clustering between the NC group and those received HFD, indicating diet-induced metabolic shifts. (B) Partial least squares-discriminant analysis further demonstrates well-defined clustering among all three groups, with high model validity (R^2 = 0.95, Q^2 = 0.77), confirming robust discrimination of metabolic phenotypes. (C) Dot plots highlight significantly altered metabolites between group comparisons with -$\log_{10}$(p-value) ≥ 1.3 (P < 0.05) and |$\log_2$ fold change| ≥ 1, with increased (orange; "up"), decreased (blue; "down"), and non-significantly changed (gray; "NS") features. (D) UpSet plot displays the number and overlap of differentially abundant metabolites in NC vs. BB, HFD vs. BB, and NC vs. HFD comparisons, identifying metabolite shifts unique to probiotic intervention. (E) Violin plots showing the abundance ($\log_2$-transformed intensity) of five key metabolites, piericidin C1, isodeoxycholic acid , tacrolimus, limonin , and chenodeoxycholic acid. Statistical comparisons were performed using the one-way ANOVA, with P < 0.05 considered significance (* P < 0.05, ** P < 0.01, **** P < 0.0001). (F) Kyoto Encyclopedia of Genes and Genomes (KEGG) pathway enrichment analysis of differentially abundant metabolites in HFD vs. BB reveals top enriched pathways. The inner ring indicates direction of change (increased: red; decreased: blue), the middle ring shows the number of metabolite mapped to each pathway (color intensity reflects significance, $-\log_{10}(p)$, represented by the color scale), and the outer ring lists specific pathways, color-coded by pathway classification. Pathways related to metabolism are prominently enriched by probiotic supplementation.

2.5 Bifidobacterium breve B2798 Modulates the Serum Metabolomic Profile and Restores Metabolic Homeostasis in High-Fat Diet-Fed Mice

To investigate the systemic metabolic effects of *B. breve* B2798 supplementation, untargeted metabolomic profiling was performed on serum samples from the three groups. Both principal component analysis and partial least squares discriminant analysis revealed clear separation among the three groups, indicating distinct global metabolic states driven by diet and probiotic intervention (Figure 5A and 5B). Volcano plot analysis identified numerous metabolites significantly altered in the BB group relative to the HFD group. In positive ion mode, 181 metabolites increased and 193 decreased; in negative ion mode, 103

increased and 136 decreased (Figure 5C), reflecting widespread modulation of circulating metabolites by probiotic treatment. A Venn diagram further highlighted the uniqueness of these changes, revealing 19 differential metabolites specifically altered in the HFD vs BB group comparison (Figure 5D).

Quantitative analysis revealed that serum levels of azelaic acid, syringic acid, and ethyl gallate were significantly elevated in the BB group compared to the HFD group ($P < 0.05$; Figure 5E). Next, KEGG pathway enrichment analysis of the differentially abundant serum metabolites between the HFD and BB groups revealed significant alterations in several key metabolic pathways. Most notably, butanoate metabolism, arginine biosynthesis, and primary bile acid biosynthesis were among the most enriched pathways (Figure 5F).

These findings indicate that *B. breve* B2798 not only reshapes the gut microbiota and fecal metabolome but also exerts systemic effects by modulating circulating metabolites and critical metabolic pathways.

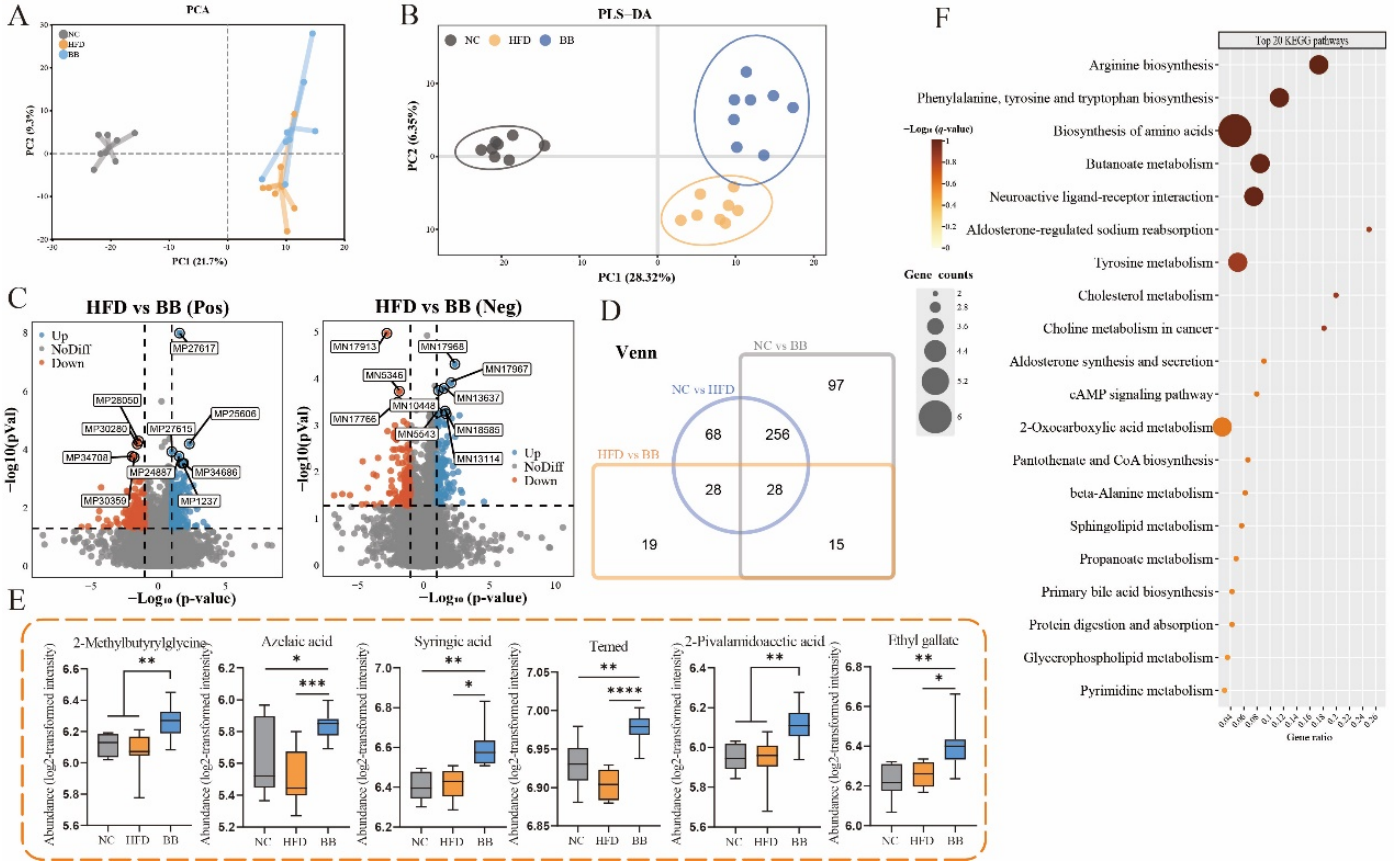

Figure 5. Serum metabolomic analysis demonstrates metabolic remodeling by *Bifidobacterium breve* B2798 in high-fat diet-fed mice. Untargeted metabolomic analysis was conducted on serum samples from the normal chow (NC), high-fat diet (HFD), and HFD supplemented with *B. breve* B2798 (BB) groups (n = 8 per group). (A) Principal component analysis (PCA) reveals distinct global metabolic profiles between the NC and the HFD-fed groups, indicating diet-induced metabolic alterations. (B) Partial least squares-discriminant analysis (PLS-DA) confirms robust group separation, supporting significant metabolic divergence among groups. (C) Volcano plots highlight differentially abundant serum metabolites between HFD and BB groups under positive (left) and negative (right) ionization modes; significance thresholds were set at $-\log_{10}$ (*p*-value) ≥ 1.3 (~ $P < 0.05$) and $|\log_2$ fold change$| \geq 1$. Blue (Up), red (Down), and gray (NoDiff) dots represent significantly increased, decreased, and non-significantly changed metabolites, respectively. (D) Venn diagram displays the number of shared and unique differential metabolites across pairwise comparisons, identifying metabolite shifts specifically associated with B2798 intervention. (E) Boxplots show relative abundances of key differential metabolites across groups. Statistical comparisons were performed using the one-way ANOVA, with $P < 0.05$ considered significance (* $P < 0.05$, ** $P < 0.01$, *** $P < 0.001$, **** $P < 0.0001$). (F) Kyoto Encyclopedia of Genes and Genomes (KEGG) pathway enrichment analysis of differential metabolites between the HFD and BB groups reveals the top 20 significantly altered pathways. The color scale represents $-\log_{10}$ (*q*-value), and the circle size indicates metabolite counts mapped to each pathway.

2.6 Integrated Multi-Omics Correlation Analysis Reveals Microbiota-Metabolite-Phenotype Interactions Underlying the Protective Effects of B. breve B2798

To gain a systems-level understanding of how *B. breve* B2798 exerts its metabolic benefits, an integrative correlation analysis was performed to link gut microbiota, fecal and serum metabolites, and key phenotypic parameters.

First, microbial co-occurrence networks were constructed based on Pearson correlation coefficients for the HFD and BB groups (Figure 6A). In the HFD group, the most highly connected taxa, based on node degree, included *Lachnospiraceae bacterium*, *Duncaniella freteri*, *Adlercreutzia mucosicola*, and *Rikenellaceae bacterium*, suggesting their potential roles as hubs in a dysbiotic microbial community associated with obesity. In contrast, the BB group exhibited a distinct network topology, with *Enterorhabdus* sp. P55, *Adlercreutzia equolifaciens*, *Anaerotruncus* sp. 1XD42_93, *Clostridium* SGB40327, and *Bacteroidaceae bacterium* emerging as central nodes, indicating a probiotic-driven restructuring toward a potentially healthier microbial interactome.

Then, pairwise Spearman correlation analyses were conducted across multi-omics datasets and phenotypic traits to identify key associations (Figure 6B). Notably, body weight, weight gain, eWAT, and iWAT showed significant negative correlations with bacterial species such as *Limosilactobacillus reuteri* and *Schaedlerella arabinosiphila*, reinforcing their association with leanness and metabolic health. *Limosilactobacillus reuteri* was also negatively correlated with fecal bile acids including ursodeoxycholic acid and taurocholic acid, but positively associated with microbial metabolites such as D-proline, acrylic acid, and tryptophan, suggesting its involvement in amino acid and organic acid metabolism.

At the metabolite level, linoleate (a polyunsaturated fatty acid) exhibited strong negative correlations with several serum metabolites linked to metabolic stress, including succinic acid, indolelactic acid, malonic acid, 3-hydroxybutyric acid, and 4-hydroxybutyric acid, while showing positive associations with essential amino acids such as L-lysine and L-methionine. This suggests that linoleate may serve as a marker of improved metabolic status and microbial metabolic activity.

Notably, succinic acid, a key intermediate in microbial fermentation and host energy metabolism, was inversely correlated with eWAT mass, but positively correlated with BAT, implicating it in the regulation of adipose tissue distribution and thermogenic activity. Similarly, tryptophan, a precursor for serotonin and microbial tryptophan metabolites (such as indoles), was positively associated with BAT, further supporting a link between microbial amino acid metabolism and energy expenditure.

Finally, KEGG functional annotation of differentially abundant metabolites in fecal and serum samples revealed a broad impact on biological pathways (Figure 6C).

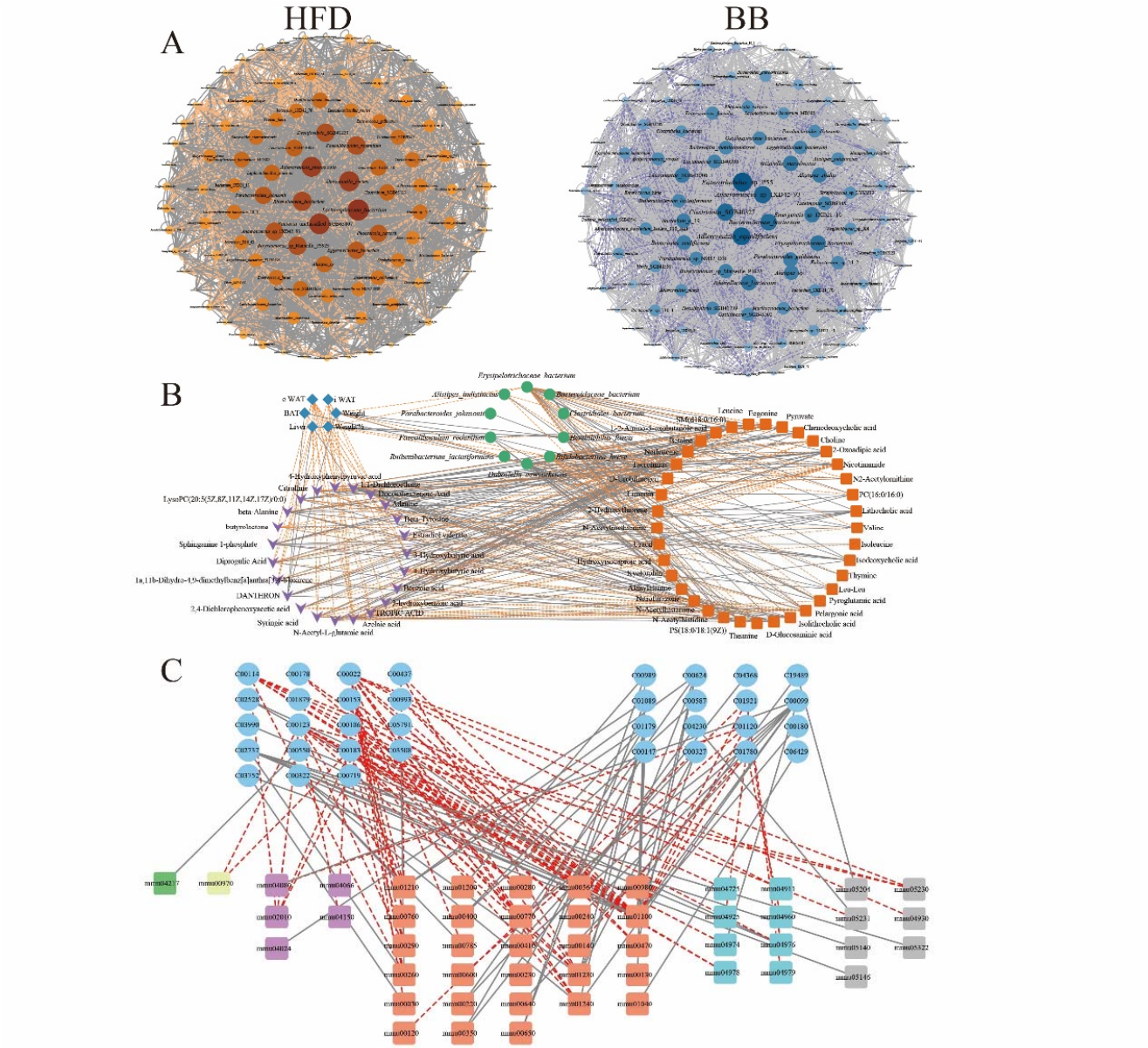

Figure 6. Integrated network analysis reveals microbial-metabolite-phenotype interactions underlying the metabolic benefits of *Bifidobacterium breve* B2798. Multi-omics network analysis was performed on the high-fat diet (HFD) and HFD supplemented with *B. breve* B2798 (BB) groups (n = 8 per group). (A) Microbial co-occurrence networks in the HFD and BB groups based on Pearson correlation analysis ($|r| > 0.5$). Nodes represent bacterial taxa, with size proportional to node degree (connectivity). In the HFD group, gray edges represent positive correlations and yellow edges negative correlations; in the BB group, gray edges denote positive and purple edges negative correlations. (B) Multi-omics interaction network integrating phenotypic parameters (e.g., body weight, adipose tissue mass), differentially abundant fecal microbes, fecal metabolites, and serum metabolites between the HFD and BB groups (all $|r| > 0.5$). Gray lines denote positive correlations; yellow lines denote negative correlations. (C) Correlation network between differential fecal and serum metabolites and enriched Kyoto Encyclopedia of Genes and Genomes (KEGG) pathways. Pathways are color-coded by functional category: green (Cellular Processes), light green (Genetic Information Processing), purple (Environmental Information Processing), orange (Metabolism), blue (Organismal Systems), and gray (Human Diseases). Gray solid lines denote positive correlations; red dashed lines indicate negative correlations. The dominance of metabolic pathways (orange) and their strong links to key metabolites underscore the central role of metabolic reprogramming in the anti-obesity effects of probiotic interventi.

After merging the top 30 annotated pathways from fecal and serum metabolomics (which included a number of overlapping pathways), a total of 50 unique pathways were obtained for network analysis. These pathways were categorized into six major functional domains: Metabolism was the most dominant (encompassing 28 pathways), followed by Organismal Systems (8), Human Diseases (7), Environmental

Information Processing (5), Cellular Processes (1), and Genetic Information Processing (1). Within the metabolic pathways, 26 differential metabolites were mapped to biosynthesis of amino acids (eight metabolites), 2-oxocarboxylic acid metabolism (seven metabolites), biosynthesis of cofactors (six metabolites), and glycine, serine and threonine metabolism (five metabolites). These pathways are central to microbial fermentation, energy production, redox balance, and host-microbe signaling, underscoring the systemic metabolic reprogramming induced by *B. breve* B2798.

Collectively, this integrative analysis reveals a complex but coherent network in which *B. breve* B2798 reshapes the gut microbiota, modulates key microbial and host metabolites, and ultimately improves metabolic phenotypes. The strong correlations between specific taxa (such as *Limosilactobacillus reuteri*), bioactive metabolites (such as succinate, tryptophan, linoleate), and adipose tissue dynamics highlight potential mechanistic links through which this probiotic strain alleviates diet-induced obesity.

3. Discussion

This study demonstrates that supplementation with *B. breve* B2798 exerts significant protective effects against HFD-induced obesity in a mouse model. Daily oral administration of *B. breve* B2798 attenuated body weight gain, reduced visceral adiposity, improved hepatic steatosis, and restored key metabolic parameters. These beneficial outcomes were accompanied by profound remodeling of the gut microbiota and systemic metabolic reprogramming, as revealed by integrated multi-omics analyses of fecal and serum metabolites (Figure 7). Our findings highlight *B. breve* B2798 as a promising probiotic candidate for the prevention and management of obesity and associated metabolic disorders.

Obesity was robustly induced by a 60% HFD, as evidenced by progressive weight gain and increased adipose tissue mass in the HFD group compared to the NC control. Notably, mice receiving *B. breve* B2798 exhibited significantly lower body weight by week 12, with no significant difference from the NC group, indicating that the probiotic effectively counteracted diet-induced weight gain. This was further supported by reduced weights of inguinal and epididymal white adipose tissues and improved liver morphology, with markedly less lipid accumulation. Histological analysis revealed that *B. breve* B2798 preserved adipocyte size, maintained multilocular architecture in BAT, and alleviated hepatic steatosis, collectively suggesting enhanced lipid homeostasis and contributing to improved tissue morphology, suggestive of preserved tissue function in adipose and liver tissues.

Serum lipid profiling yielded unexpected yet mechanistically informative results. Contrary to typical obesity-associated dyslipidemia, the HFD group exhibited lower TC and TG levels than the NC group. While this may seem paradoxical, prolonged HFD feeding can lead to hepatic lipid overload and impaired lipoprotein secretion, resulting in reduced circulating lipids despite systemic lipid accumulation, a phenomenon observed in murine models of non-alcoholic fatty liver disease where hepatic very-low-density lipoprotein export becomes limited[12]. Notably, *B. breve* B2798 intervention reversed this pattern, significantly increasing HDL-C levels and moderately elevating TC. The rise in HDL-C, a well-established marker of cardiovascular protection[13], suggests improved reverse cholesterol transport and enhanced hepatic lipid

export. These changes imply that *B. breve* B2798 may help restore hepatic metabolic function, facilitating the mobilization and clearance of stored lipids, thereby reducing ectopic fat deposition.

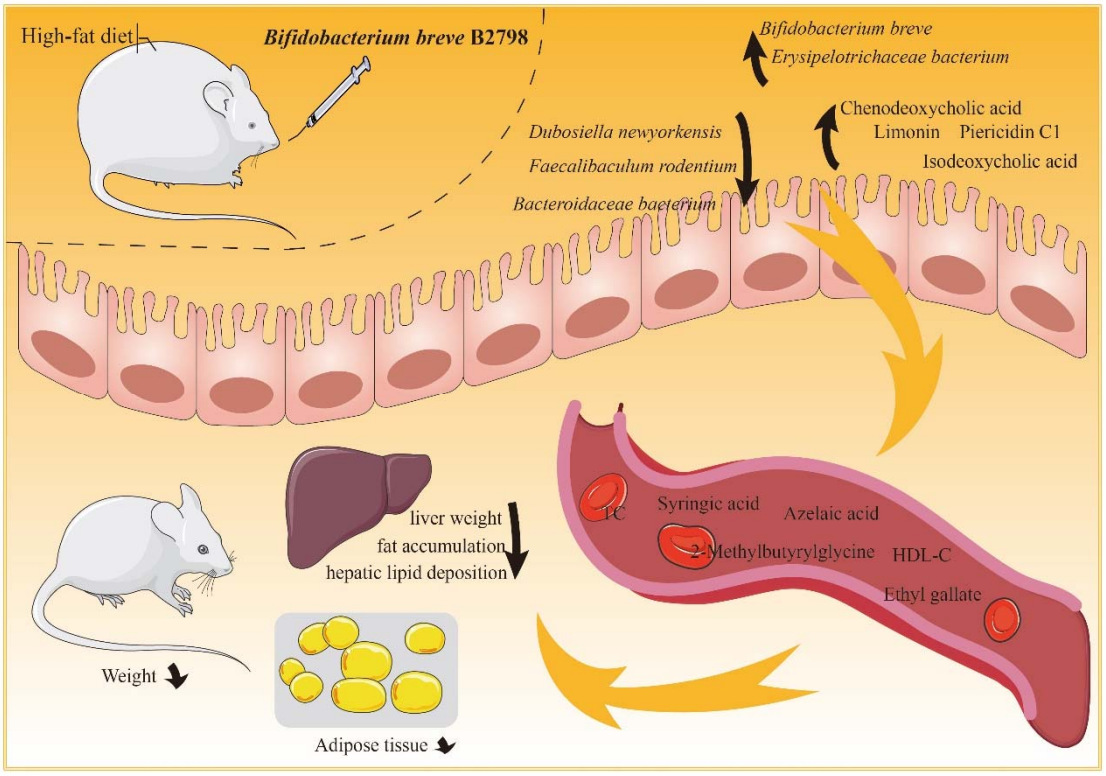

Figure 7. Schematic illustration of the effects of *Bifidobacterium breve* B2798 on high-fat diet–induced metabolic disorders in mice. Oral administration of B. breve B2798 modulates gut microbiota composition (e.g., increased *Bifidobacterium breve*, *Erysipelotrichaceae bacterium*; altered levels of *Dubosiella newyorkensis*, *Faecalibaculum rodentium*, and *Bacteroidaceae bacterium*) and bile acid metabolites (chenodeoxycholic acid, limonin, piericidin C1, isodeoxycholic acid). These changes influence host circulating metabolites (syringic acid, azelaic acid, methylbutyrylglycine, ethyl gallate, HDL-C), thereby reducing body weight, adipose tissue mass, liver weight, fat accumulation, and hepatic lipid deposition.

The gut microbiota plays a pivotal role in host energy balance and metabolic health, and HFDs are known to disrupt microbial community structure, which is mitigated by probiotic intervention[14]. Consistent with prior research[15], our results showed that an HFD led to a significant increase in microbial α-diversity, as indicated by increased Shannon and Simpson indices, reflecting diet-induced dysbiosis. Although *B. breve* B2798 intervention did not fully restore overall microbial diversity, it induced a distinct shift in β-diversity, forming a unique microbial cluster separate from both NC and HFD groups. This indicates that the probiotic exerts a strong, specific influence on community composition, independent of general diversity metrics.

Taxonomic analysis revealed that *B. breve* B2798 supplementation significantly increased the abundance of *Eubacteriales* unclassified and *Erysipelotrichaceae* unclassified, members of the Firmicutes phylum with potential metabolic benefits. *Eubacteriales* includes butyrate-producing species known to enhance gut barrier integrity and reduce inflammation[16]. Additionally, STAMP analysis found a significant increase in *Bifidobacterium breve* abundance in the BB group, possibly the administered strain though further confirmation is needed. Concurrently, *B. breve* B2798 supplementation elevated the levels of beneficial taxa, such as *Clostridiales bacterium* while reducing the intestinal abundance of *Erysipelotrichaceae bacterium*. Notably, *Clostridiales bacterium* has been reported to prevent weight gain by impairing intestinal lipid

absorption[17]. Furthermore, prior studies have shown that the proportion of *Erysipelotrichi* and *Bacilli* within the Firmicutes phylum is significantly higher in high-fat/high-sugar diet groups compared to controls[18]. These observations suggest that *B. breve* B2798 intervention may promote a broader ecological shift toward a healthier microbiome.

These microbial changes were mirrored by significant alterations in the fecal metabolome. Specifically, *B. breve* B2798 supplementation significantly increased levels of bioactive gut metabolites, including limonin, chenodeoxycholic acid, piericidin C1, andisodeoxycholic acid , all of which are associated with anti-obesity effects or important physiological benefits. Limonin has been shown to reduce fat accumulation and body weight gain while alleviating HFD-induced hepatic steatosis and hyperlipidemia in animal models[19]. Chenodeoxycholic acid activates the TGR5 receptor, promoting energy expenditure and inhibiting adipogenesis through suppression of peroxisome proliferator-activated receptor gamma (PPARγ)[20]. Piericidin C1, though less studied in the context of glucose and lipid metabolism, may contribute to microbial community regulation through its antimicrobial properties, potentially suppressing pathobionts[21]. Additionally, while deoxycholic acid has been shown to reduce HFD-induced obesity by enhancing lipid catabolism and significantly lowering fat mass[22], the specific effects of isodeoxycholic acid remains unclear. These results underscore the ability of *B. breve* B2798 to promote a more favorable microbial and metabolic environment.

Pathway analysis revealed that *B. breve* B2798 modulated key metabolic pathways, including 2-oxocarboxylic acid metabolism, amino acid biosynthesis, and pantothenate and CoA biosynthesis, all critical for microbial energy production and host coenzyme availability. Notably, the biosynthesis of branched-chain amino acids (BCAAs), valine, leucine, and isoleucine, was downregulated in the BB group. Elevated circulating BCAAs are strongly linked to obesity, insulin resistance, and type 2 diabetes mellitus[23], and their microbial production may exacerbate metabolic dysfunction. By reducing BCAA biosynthesis, *B. breve* B2798 may help mitigate this risk, aligning with prior research showing that BCAA restriction improves metabolic health via reducing body weight and intestinal Firmicutes/Bacteroidetes ratio[24].

Serum metabolomics further revealed systemic benefits. *Bifidobacterium breve* B2798 supplementation increased circulating levels of azelaic acid, syringic acid, and ethyl gallate, metabolites with anti-inflammatory, antioxidant, and anti-adipogenic properties. Azelaic acid, a dicarboxylic acid derived from gut microbial oxidation of dietary unsaturated fatty acids, has been linked to improved anti-inflammatory effects, insulin sensitivity, and glucose and lipid metabolism[25]. Syringic acid reduces visceral fat and insulin resistance in HFD-fed mice[26]; and ethyl gallate modulates protein tyrosine phosphatase non-receptor type 6 and PPARγ[27]. These compounds likely originate from microbial metabolism or enhanced dietary polyphenol biotransformation[28-30], suggesting enhanced microbial production or host absorption of beneficial phytochemicals in the presence of *B. breve* B2798 and underscoring the gut-liver axis in probiotic action.

The results of KEGG analysis of serum metabolites highlighted enrichment in butanoate (butyrate) metabolism, arginine biosynthesis, and primary bile acid biosynthesis. Butanoate metabolism is central to gut

barrier integrity, anti-inflammatory response, and systemic energy metabolism[31-32], while arginine metabolism influences nitric oxide signaling[33]. The modulation of primary bile acid biosynthesis further suggests that *B. breve* B2798 may influence enterohepatic circulation and lipid metabolism through host-microbe crosstalk[34]. The positive correlation between succinic acid and BAT, along with its inverse association with eWAT, suggests a role in promoting thermogenesis and redistributing fat storage. Similarly, tryptophan, a precursor for neuroactive and immunomodulatory metabolites, was positively correlated with BAT, further linking microbial amino acid metabolism to energy expenditure.

While our metabolomic analyses identified changes in bile acids and other metabolites predicted to activate TGR5 and PPARγ signaling, direct measurement of receptor expression or downstream target genes in relevant tissues (e.g., adipose, liver) was not performed in this study. Future work should include targeted qPCR or Western blot analysis of key pathway components to functionally validate these predicted mechanisms.

Integrated correlation analysis revealed a complex network of interactions linking gut microbial taxa, metabolite profiles, and host phenotypic outcomes. Notably, *Limosilactobacillus reuteri* and *Schaedlerella arabinosiphila* were negatively correlated with adiposity, reinforcing their roles in metabolic health. The strong inverse association between fecal linoleate and multiple serum organic acids, such as succinic acid, malonic acid, and 3-hydroxybutyric acid, suggests improved systemic lipid metabolism and reduced metabolic stress in the probiotic-treated group. Furthermore, 3-hydroxybutyrate, a key ketone body and signaling molecule, was negatively correlated with fat mass, supporting its role in energy homeostasis[35]. These correlations highlight a functional gut-microbiota-host axis that contributes to the anti-obesity effects of *B. breve* B2798.

Despite its strengths, this study has several limitations. First, while we observed significant metabolic improvements, the precise molecular mechanisms, such as direct microbial-host signaling, immune modulation, or bile acid receptor activation, remain to be fully elucidated. Second, although we demonstrated potential strain colonization via increased *Bifidobacterium breve* abundance, long-term engraftment and functional persistence beyond the intervention period were not assessed. Finally, the functional validation of key metabolites (such as piericidin C1,isodeoxycholic acid) and their causal roles in metabolic improvement requires further investigation using gnotobiotic models or metabolite supplementation studies.

It is also important to note that the beneficial effects observed in this study are likely strain-specific. Not all *Bifidobacterium* strains confer metabolic benefits; some have even been associated with adverse outcomes in certain contexts[36]. The unique genomic and metabolic features of *B. breve* B2798, such as its ability to modulate bile acid metabolism or produce specific bioactive compounds, may underlie its efficacy, highlighting the importance of precise strain selection in probiotic development.

Collectively, our data suggest a potential mechanism in which *B. breve* B2798 reshapes the gut microbiota to favor taxa that produce beneficial metabolites, such as secondary bile acids, SCFA precursors, and bioactive phenolics, which in turn signal through host receptors (such as TGR5, PPARγ) to regulate lipid

metabolism, inflammation, and energy expenditure. This gut-microbiota-liver-adipose axis may underlie the systemic metabolic improvements observed in the BB group.

We acknowledge that direct evidence linking gut microbiota alterations to improvements in liver and systemic metabolism is lacking in the current study. Specifically, the absence of intestinal barrier function indicators-such as plasma LPS levels, tight junction protein expression, or colonic histological assessment-limits our ability to conclusively demonstrate that gut-derived signals are responsible for the metabolic improvements in distal organs. These measurements will be critical in future studies to complete the mechanistic chain.

In conclusion, our study provides compelling evidence that *B. breve* B2798 ameliorates HFD-induced obesity through a multi-faceted mechanism: reshaping the gut microbiota toward a beneficial composition, enhancing the production of health-promoting metabolites, modulating key metabolic pathways, and improving systemic metabolic health. These findings not only expand our understanding of probiotic-host interactions but also support the development of microbiome-targeted strategies for combating obesity and metabolic syndrome. Future studies should employ fecal microbiota transplantation and metabolite supplementation to establish causality, and investigate tissue-specific molecular mechanisms including thermogenesis, inflammation, and lipid metabolism in adipose and liver. Assessment of intestinal barrier function is also needed to confirm that gut-derived signals mediate distal organ improvements. Dose-response studies, long-term safety evaluations, and ultimately human trials will be essential to translate these findings into clinical applications.

4. Conclusion

Bifidobacterium breve B2798 effectively mitigates HFD-induced obesity in mice by modulating the gut microbiota and restoring metabolic homeostasis. The probiotic intervention reduced adiposity, improved liver health, and enhanced systemic metabolic profiles through microbial remodeling and the enrichment of beneficial metabolites. These findings highlight the therapeutic potential of strain-specific probiotics in managing obesity and related metabolic disorders.

5. Materials and Methods

5.1 Ethics Statement

All experimental procedures involving animals were conducted in accordance with the Guide for the Care and Use of Laboratory Animals published by the U.S. National Institutes of Health and were approved by the Animal Ethics Committee of Inner Mongolia Agricultural University (Approval No: NND2023097).

5.2 Probiotic Strain

The probiotic strain used in this study, *B. breve* B2798, was originally isolated and preserved in the culture collection of the Laboratory of Dairy Biotechnology and Engineering, Inner Mongolia Agricultural University. Prior to administration, the strain was revitalized and subjected to high-density fermentation under anaerobic conditions. Following fermentation, the bacterial cells were harvested, suspended in a

cryoprotectant solution, and lyophilized to produce a stable powder formulation. The viability of the freeze-dried powder was assessed using the spread-plate method on agar under anaerobic conditions, and results were further confirmed by flow cytometry to ensure accuracy. The final product contained approximately 2×10^9 CFU/mL. For daily gavage, the lyophilized powder was freshly reconstituted in sterile 0.9% saline immediately before administration to maintain bacterial viability.

5.3 Animals and Diets

A total of twenty-four male C57BL/6 mice, aged six weeks, were purchased from Beijing Huafukang Bioscience Co., Ltd. (Beijing, China). Upon arrival, the animals were housed in a specific pathogen-free facility at the Laboratory of Dairy Biotechnology and Engineering, Inner Mongolia Agricultural University, under strictly controlled environmental conditions: a constant temperature of 20-26 °C, relative humidity of 40%-60%, and a 12-h light/dark cycle. All mice were allowed free access to food and autoclaved drinking water throughout the study.

Prior to the initiation of the experiment, the mice underwent a one-week acclimatization period during which they were fed a standard chow diet to minimize environmental stress and ensure physiological stability. The diet-induced obesity model was established based on previously described methods [39-40] with modifications. The experimental diets were provided by Trophic Animal Feed High-Tech Co., Ltd. (Nantong, China).Two diets were used: a standard chow diet (TP23302) for the NC group, and a 60% HFD (TP23300) administered to both the HFD and BB groups. The macronutrient composition of the diets was isocaloric except for fat content, ensuring that any observed effects could be attributed to dietary fat or intervention rather than caloric disparity.

5.4 Experimental Design

Following a one-week acclimatization, the 24 male C57BL/6 mice were randomly assigned to one of three experimental groups (n = 8 per group): the NC group, fed a standard chow diet; the HFD group, fed a 60% fat diet; and the BB intervention group, which received the same HFD as the HFD group but was additionally supplemented with the probiotic strain. Randomization was performed to ensure uniformity in initial body weights across groups.

Starting on Day 1, mice in the NC and HFD groups received daily oral gavage of 0.1 mL sterile saline, while the BB group received 0.1 mL of saline containing *B. breve* B2798 at a dose of 2×10^9 CFU per mouse. Body weight was recorded biweekly throughout the experimental period to monitor changes in growth and adiposity. At the end of the experiment, fresh fecal samples were collected and immediately snap-frozen in liquid nitrogen, and stored at –80 °C for subsequent gut microbiota and metabolic analyses. Blood samples were collected via retro-orbital plexus puncture under isoflurane anesthesia using a capillary tube. Serum was separated by centrifugation and stored at –80 °C for biochemical assays. Following blood collection, mice were euthanized by cervical dislocation in accordance with approved ethical guidelines. Key metabolic tissues, including iWAT, eWAT, BAT, and liver, were rapidly excised and stored appropriately for further analyses.

5.5 Histopathological Analysis

Following euthanasia, key metabolic tissues were rapidly excised and processed for histopathological examination. Epididymal white adipose tissue, iWAT, interscapular BAT, and liver tissues were collected from each mouse. All samples were immediately fixed in 4% paraformaldehyde for 24-48 h at 4 °C to ensure optimal preservation of tissue architecture, followed by routine processing for paraffin embedding. Tissue sections were cut using a microtome and mounted on glass slides. Adipose tissue sections were stained with hematoxylin and eosin to assess adipocyte size, morphology, and overall tissue structure. Liver sections were stained with oil red O on frozen sections to visualize neutral lipid accumulation, as this stain specifically highlights TG-rich lipid droplets in hepatocytes. All stained sections were examined under a light microscope at appropriate magnifications.

Based on the protocol described in Reference [41], the relative lipid droplet area was quantified using ImageJ software on random microscopic fields (40×) per section. The quantified values were then normalized to the mean value of the HFD group (set as 100%) for statistical analysis.

5.6 Serum Biochemical Analysis

Serum biochemical parameters were analyzed to evaluate lipid metabolism and liver function in the experimental mice. Levels of TG, TC, HDL-C, and LDL-C were measured using a Hitachi 3100 automated biochemistry analyzer (Hitachi High-Technologies Corporation, Tokyo, Japan). Triglyceride concentrations were determined using the glycerol-3-phosphate oxidase-peroxidase enzymatic method. Total cholesterol was quantified via the cholesterol oxidase-peroxidase enzymatic assay. The level of HDL-C was measured using a direct method based on selective inhibition of non-HDL lipoproteins, while LDL-C was assessed using a direct surfactant-based clearance method that selectively solubilizes lipoproteins. All assays were performed according to the manufacturer's instructions provided with the respective commercial kits (using kits from Leadman Biochemistry Co., Ltd.).

5.7 Fecal Metagenomic Sequencing

Total genomic DNA was extracted from fecal samples using the QIAamp Fecal DNA Extraction Kit (Qiagen, Hilden, Germany), following the manufacturer's instructions. The quality, purity, and concentration of the extracted DNA were assessed using multiple complementary methods: DNA integrity was evaluated by 0.6% agarose gel electrophoresis; purity was determined via UV spectrophotometry using the Nanodrop One (Thermo Fisher Scientific, Inc., Waltham, MA, USA), with acceptable samples exhibiting an A260/A280 ratio between 1.8 and 2.0; and the DNA concentration was quantified with the Invitrogen Qubit™ dsDNA HS (High Sensitivity) Assay Kit (Thermo Fisher Scientific, Inc., Waltham, MA, USA). Only samples meeting stringent quality criteria, DNA concentration > 1 μg, absence of degradation, and low contamination, were selected for downstream library preparation and sequencing.

Library construction was performed using the NEBNext® Ultra™ DNA Library Prep Kit for Illumina® (New England Biolabs, Ipswich, MA, USA), according to the manufacturer's instructions. Briefly, 1 μL of high-quality genomic DNA was fragmented to an average size of approximately 350 bp using the Covaris

M220 Focused-ultrasonicator (Covaris LLC, Woburn, MA, USA). The fragmented DNA underwent end repair, 3' adenylate tailing, and ligation of Illumina-compatible sequencing adapters. Adapter-ligated fragments were amplified by PCR to enrich the library, followed by purification using the AMPure XP magnetic beads (Beckman Coulter, Inc., Brea, CA, USA) to remove unincorporated primers and short fragments. The final library insert size distribution was validated on the Agilent 2100 Bioanalyzer (Agilent Technologies, Inc., Santa Clara, CA, USA). Library concentration was accurately measured by quantitative PCR. Qualified libraries were pooled and sequenced on the Illumina NovaSeq 6000 platform (Illumina, San Diego, CA, USA) to generate 150-bp paired-end reads.

Raw sequencing data were subjected to comprehensive quality control using Trimmomatic from KneadData pipeline (http://huttenhower.sph.harvard.edu/kneaddata), which removed low-quality bases, adaptors, and contaminant sequences. Host-derived sequences were then filtered out by aligning the cleaned reads to the mouse reference genome using the Bowtie2 with default parameters, retaining only non-host microbial reads for downstream analysis. Taxonomic profiling of the gut microbiota was performed using MetaPhlAn2[37]. Functional potential of the gut microbial community was inferred using HUMAnN2[38]. All bioinformatic analyses were conducted using standardized pipelines to ensure reproducibility and biological relevance of the metagenomic data.

5.8 Untargeted Metabolomic Analysis of Fecal and Serum Samples

5.8.1 Fecal Sample Pretreatment

Fecal samples were thawed gradually on ice at 4 °C. For each sample, 200 mg of homogenized fecal material was accurately weighed and transferred into a 2 mL centrifuge tube. To this, 600 μL of pre-chilled methanol containing 4 ppm of L-2-chlorophenylalanine (used as an internal standard for normalization and quality control) was added. The mixture was vortexed vigorously for 30 s to ensure thorough mixing. To enhance cell lysis and improve metabolite extraction efficiency, a small number of 3 mm zirconia beads were added to each tube. The samples were then homogenized using a tissue grinder at a frequency of 50 Hz for 2 min. Following homogenization, the samples were subjected to ultrasonication in an ice-cooled ultrasonic bath for 10 min at room temperature to further disrupt microbial and host cellular components and facilitate metabolite release. After sonication, the samples were centrifuged at 12,000 rpm for 10 min at 4 °C to pellet insoluble debris. The resulting supernatants were carefully collected and filtered through a 0.22 μm membrane filter. Filtered supernatants were transferred into autosampler vials for metabolomic analysis. Additionally, equal volumes of supernatant from each sample were pooled and used as a quality control sample, which was analyzed repeatedly throughout the analytical batch sequence to assess instrument stability and ensure data reproducibility and reliability.

5.8.2 Serum Sample Pretreatment

Serum samples were thawed at 4 °C and vortexed vigorously for 1 min to ensure homogeneity. An aliquot of 100 μL of serum was transferred into a 2 mL centrifuge tube, followed by the addition of 400 μL of ice-cold methanol. The mixture was vortexed again for 1 min to precipitate proteins and facilitate metabolite

extraction. After incubation at -20 °C for 30 min to enhance protein precipitation, the samples were centrifuged at 12,000 rpm for 10 min at 4 °C. The supernatant was carefully transferred to a new 2 mL tube and dried under vacuum. The resulting metabolite-containing residue was reconstituted in 150 μL of 80% methanol (v/v in water, containing 4 ppm L-2-chlorophenylalanine). The reconstituted solutions were filtered through a 0.22 μm membrane filter and transferred into autosampler vials for subsequent analysis. To ensure analytical consistency and monitor system performance, a quality control sample was generated by pooling an equal volume of supernatant from each individual serum sample. This pooled quality control sample was injected repeatedly at regular intervals throughout the analytical run sequence to evaluate instrument stability.

5.8.3 Chromatographic and Mass Spectrometric Conditions

Chromatographic separation was performed using an ACQUITY UPLC HSS T3 column (2.1 mm × 100 mm, 1.8 μm; Waters Corporation, Milford, MA, USA), maintained at 40 °C. The mobile phases consisted of: (A) ultrapure water containing 0.1% formic acid for positive ion mode or 5 mM ammonium formate in water for negative ion mode; and (B) acetonitrile with 0.1% formic acid (positive mode) or pure acetonitrile (negative mode). The flow rate was set at 0.3 mL/min, and the injection volume was 2 μL. A gradient elution program was applied for both ionization modes as follows: 0-1 min, 8% B (isocratic); 1-8 min, linear increase from 8% to 98% B; 8-10 min, 98% B (hold); 10-10.1 min, ramp down to 8% B; and 10.1-12 min, 8% B (re-equilibration). This gradient ensured efficient separation of a broad range of polar and nonpolar metabolites within a short runtime while maintaining excellent peak resolution and reproducibility.

Mass spectrometric detection was performed using an Orbitrap Exploris 120 mass spectrometer (Thermo Fisher Scientific, Inc., Waltham, MA USA) equipped with an electrospray ionization source. The instrument was operated in both positive and negative ion modes, with polarity switching enabled for comprehensive metabolite coverage. Ion source parameters were optimized as follows: spray voltage was set to 3.50 kV in positive mode and −2.50 kV in negative mode; sheath gas and auxiliary gas flow rates were 40 and 10 arbitrary units, respectively; capillary temperature was maintained at 325 °C. Full-scan MS data were acquired in the Orbitrap analyzer at a resolution of 60,000 over a mass range of m/z 100-1,000. For MS/MS acquisition, the top four most intense ions from each full scan were selected for fragmentation using higher-energy collisional dissociation with a normalized collision energy of 30%. MS/MS spectra were recorded at a resolution of 15,000. A dynamic exclusion strategy was applied to prevent repeated fragmentation of the same precursor ions, thereby enhancing the depth of metabolite identification.

Raw data files were converted to the open mzXML format using MSConvert (ProteoWizard toolkit, version 3.0.24263-36e7380) for compatibility with downstream processing tools. Data preprocessing, including retention time correction, peak detection, deconvolution, integration, alignment, and noise filtering, was performed using the XCMS package (version 4.2.3). Metabolite identification was based on accurate mass, retention time, and MS/MS fragmentation patterns. Putative identifications were made by matching experimental data against an in-house spectral library and public databases, including the Human Metabolome Database (HMDB), METLIN, MassBank, and mzCloud.

5.9 Statistical Analysis

All statistical analyses and data visualizations were performed using R(version 4.4.1), GraphPad Prism (version 9), and Adobe Illustrator (version 2020) for final figure refinement. Data are presented as mean ± standard deviation unless otherwise specified. For comparisons between two groups, the non-parametric Wilcoxon rank-sum test (Mann-Whitney test) was used when data deviated from normality or exhibited unequal variances. For comparisons among three or more groups, one-way analysis of variance (ANOVA) applied. All tests were two-tailed, and a p-value of < 0.05 was considered statistically significant. To assess global differences in gut microbial community composition, principal coordinates analysis was performed based on Bray-Curtis distances. Spearman's rank correlation coefficient was employed to evaluate associations between gut microbiota taxa and various host metabolic parameters.

Funding

This work was supported by the Program for Young Talents of Science and Technology in Universities of Inner Mongolia Autonomous Region (NJYT22036）, National Natural Science Foundation of China (32325040, U22A20540), Basic Research Operating Expenses Program for Colleges, Universities directly under the Inner Mongolia Autonomous Region (BR22–14–01), the earmarked fund for CARS36, and the Natural Science Foundation of Inner Mongolia Autonomous Region Project (2024QN03050).

Conflicts of Interest

The authors declare that they have no known competing financial interest or personal relationships that could have appeared to influence the work reported in this paper.

Data Availability Statement

The sequencing data generated in this study have been deposited in the China National GeneBank Database (CNSA) under accession number CNP0008039.

References

[1] United Nations Children's Fund. Child Nutrition Report 2025: Feeding Profit: How Food Environments Are Failing Children. UNICEF, 2025..

[2] Di Vincenzo F, Del Gaudio A, Petito V, et al. Gut microbiota, intestinal permeability, and systemic inflammation: a narrative review[J]. Internal and emergency medicine, 2024, 19(2): 275-293.

[3] Magne F, Gotteland M, Gauthier L, Zazueta A, Pesoa S, Navarrete P, Balamurugan R. The Firmicutes/Bacteroidetes Ratio: A Relevant Marker of Gut Dysbiosis in Obese Patients? Nutrients. 2020 May 19;12(5):1474. doi: 10.3390/nu12051474.

[4] Bäckhed F, Ding H, Wang T, et al. The gut microbiota as an environmental factor that regulates fat storage[J]. Proceedings of the national academy of sciences, 2004, 101(44): 15718-15723.

[5] Sekirov I, Russell SL, Antunes LC, Finlay BB. Gut microbiota in health and disease. Physiol Rev. 2010 Jul;90(3):859-904.

[6] Du W, Zou Z P, Ye B C, et al. Gut microbiota and associated metabolites: key players in high-fat diet-induced chronic diseases[J]. Gut Microbes, 2025, 17(1): 2494703.

[7] Hill, C. et al. Expert consensus document. The International Scientific Association for Probiotics and Prebiotics consensus statement on the scope and appropriate use of the term probiotic. Nat. Rev. Gastroenterol. Hepatol. 11, 506–514 (2014).

[8] Guazzelli Marques C,De Piano Ganen A,Zaccaro De Ba-rros A,et al.Weight loss probiotic supplementation effect in overweight and obesity subjects:A review[J].Clinical Nutrition,2020(3):694-704.

[9] Yadav H, Lee JH, Lloyd J, Walter P, Rane SG. Beneficial metabolic effects of a probiotic via butyrate-induced GLP-1 hormone secretion. J Biol Chem. 2013 Aug 30;288(35):25088-25097. doi: 10.1074/jbc.M113.452516. Epub 2013 Jul 8. PMID: 23836895; PMCID: PMC3757173.

[10] Ejtahed H S,Angoorani P,Soroush A R,et al.Probiotics supplementation for the obesity management:A systematic review of animal studies and clinical trials[J].Journal of Medicine & Pharmacotherapy,2020(12):191-208.

[11] Li B, Liu K, Kwok LY, et al. Development of a non-target metabolomics-based screening method for elucidating metabolic and probiotic potential of bifidobacteria. Innov Food Sci Emerg Technol. 2022;77:102971.

[12] Eccleston HB, Andringa KK, Betancourt AM, King AL, Mantena SK, Swain TM, Tinsley HN, Nolte RN, Nagy TR, Abrams GA, Bailey SM. Chronic exposure to a high-fat diet induces hepatic steatosis, impairs nitric oxide bioavailability, and modifies the mitochondrial proteome in mice. Antioxid Redox Signal. 2011 Jul 15;15(2):447-59. doi: 10.1089/ars.2010.3395.

[13] Nagao M, Nakajima H, Toh R, Hirata KI, Ishida T. Cardioprotective Effects of High-Density Lipoprotein Beyond its Anti-Atherogenic Action. J Atheroscler Thromb. 2018 Oct 1;25(10):985-993. doi: 10.5551/jat.RV17025.

[14] Du W, Zou ZP, Ye BC, Zhou Y. Gut microbiota and associated metabolites: key players in high-fat diet-induced chronic diseases. Gut Microbes. 2025 Dec;17(1):2494703.

[15] Wang, B.; Kong, Q.; Li, X.; Zhao, J.; Zhang, H.; Chen, W.; Wang, G. A High-Fat Diet Increases Gut Microbiota Biodiversity and Energy Expenditure Due to Nutrient Difference. Nutrients 2020, 12, 3197.

[16] Kalnina, I., Gudra, D., Silamikelis, I., Viksne, K., Roga, A., Skinderskis, E., ... & Klovins, J. (2023). Variations in the relative abundance of gut Bacteria correlate with lipid profiles in healthy adults. Microorganisms, 11(11), 2656.

[17] Petersen C, Bell R, Klag KA, et al. T cell–mediated regulation of the microbiota protects against obesity. Science. 2019;365(6451):eaat9351.

[18] Turnbaugh, Peter J., Vanessa K. Ridaura, Jeremiah J. Faith, Federico E. Rey, Rob Knight, and Jeffrey I. Gordon. 2009. “The Effect of Diet on the Human Gut Microbiome: A Metagenomic Analysis in Humanized Gnotobiotic Mice.” Science Translational Medicine 1: 1.

[19] Yan, Mingzhu, et al. "Limonin counteracts obesity by activating thermogenesis in brown and white adipose tissues." Journal of Functional Foods 100 (2023): 105393.

[20] Chen X, Yan L, Guo Z, et al. Chenodeoxycholic acid attenuates high-fat diet-induced obesity and hyperglycemia via the G protein-coupled bile acid receptor 1 and proliferator-activated receptor γ pathway[J]. Experimental and Therapeutic Medicine, 2017, 14(6): 5305-5312.

[21] Hayakawa, Y., Shirasaki, S., Shiba, S., Kawasaki, T., Matsuo, Y., Adachi, K. et al. (2007) Piericidins C7 and C8, new cytotoxic antibiotics produced by a marine Streptomyces sp. Journal of Antibiotics, 60, 196–200.

[22] Tuerhongjiang G, Li Y, Meng Z, et al. Deoxycholic acid ameliorates obesity and insulin resistance by enhancing lipolysis and thermogenesis[J]. Lipids in Health and Disease, 2025, 24(1): 70.

[23] Fontana, Luigi, et al. "Decreased consumption of branched-chain amino acids improves metabolic health." Cell reports 16.2 (2016): 520-530.

[24] Zhang, Lei, et al. "Dietary branched-chain amino acids restriction in high-fat diet-induced obese mice: effects on metabolic homeostasis, adipose inflammation, and gut microbiota." The Journal of Nutrition (2025).

[25] Nychyk O, Barton W, Rudolf AM, Boscaini S, Walsh A, Bastiaanssen TFS, Giblin L, Cormican P, Chen L, Piotrowicz Y, Derous D, Fanning Á, Yin X, Grant J, Melgar S, Brennan L, Mitchell SE, Cryan JF, Wang J, Cotter PD, Speakman JR, Nilaweera KN. Protein quality and quantity influence the effect of dietary fat on weight gain and tissue partitioning via host-microbiota changes. Cell Rep. 2021 May 11;35(6):109093. doi: 10.1016/j.celrep.2021.109093.

[26] Ham JR, Lee HI, Choi RY, Sim MO, Seo KI, Lee MK. Anti-steatotic and anti-inflammatory roles of syringic acid in high-fat diet-induced obese mice. Food Funct. 2016 Feb;7(2):689-97.

[27] Ahn D, Kim J, Nam G, Zhao X, Kwon J, Hwang JY, Kim JK, Yoon SY, Chung SJ. Ethyl Gallate Dual-Targeting PTPN6 and PPARγ Shows Anti-Diabetic and Anti-Obese Effects. Int J Mol Sci. 2022 Apr 30;23(9):5020.

[28] Brink LR, Mercer KE, Piccolo BD, Chintapalli SV, Elolimy A, Bowlin AK, Matazel KS, Pack L, Adams SH, Shankar K, Badger TM, Andres A, Yeruva L. Neonatal diet alters fecal microbiota and metabolome profiles at different ages in infants fed breast milk or formula. Am J Clin Nutr. 2020 Jun 1;111(6):1190-1202. doi: 10.1093/ajcn/nqaa076.

[29] Bartel I, Mandryk I, Horbańczuk JO, Wierzbicka A, Koszarska M. Nutraceutical Properties of Syringic Acid in Civilization Diseases-Review. Nutrients. 2023 Dec 19;16(1):10. doi: 10.3390/nu16010010.

[30] Ezhilarasan D, Shree Harini K, Karthick M, Selvaraj C. Ethyl gallate concurrent administration protects against acetaminophen-induced acute liver injury in mice: An in vivo and in silico approach. Chem Biol Drug Des. 2024 Jan;103(1):e14369. doi: 10.1111/cbdd.14369.

[31] Hodgkinson K, El Abbar F, Dobranowski P, Manoogian J, Butcher J, Figeys D, Mack D, Stintzi A. Butyrate's role in human health and the current progress towards its clinical application to treat gastrointestinal disease. Clin Nutr. 2023 Feb;42(2):61-75. doi: 10.1016/j.clnu.2022.10.024.

[32] Zhang L, Liu C, Jiang Q, Yin Y. Butyrate in Energy Metabolism: There Is Still More to Learn. Trends Endocrinol Metab. 2021 Mar;32(3):159-169. doi: 10.1016/j.tem.2020.12.003.

[33] Fung TS, Ryu KW, Thompson CB. Arginine: at the crossroads of nitrogen metabolism. EMBO J. 2025 Mar;44(5):1275-1293. doi: 10.1038/s44318-025-00379-3.

[34] Fleishman JS, Kumar S. Bile acid metabolism and signaling in health and disease: molecular mechanisms and therapeutic targets. Signal Transduct Target Ther. 2024 Apr 26;9(1):97. doi: 10.1038/s41392-024-01811-6.

[35] Hsu TT, et al. 3-Hydroxybutyric acid interacts with lipid monolayers at concentrations that impair consciousness. Langmuir. 2013 Feb 12;29(6):1948-55.

[36] Sarkar A, Mandal S. Bifidobacteria-Insight into clinical outcomes and mechanisms of its probiotic action. Microbiol Res. 2016 Nov;192:159-171. doi: 10.1016/j.micres.2016.07.001.

[37] Truong DT, Franzosa EA, Tickle TL, Scholz M, Weingart G, Pasolli E, Tett A, Huttenhower C, Segata N. MetaPhlAn2 for enhanced metagenomic taxonomic profiling. Nat Methods. 2015 Oct;12(10):902-3. doi: 10.1038/nmeth.3589. Erratum in: Nat Methods. 2016 Jan;13(1):101.

[38] Franzosa EA, McIver LJ, Rahnavard G, Thompson LR, Schirmer M, Weingart G, Lipson KS, Knight R, Caporaso JG, Segata N, Huttenhower C. Species-level functional profiling of metagenomes and metatranscriptomes. Nat Methods. 2018 Nov;15(11):962-968. doi: 10.1038/s41592-018-0176-y.

[39] Zhu L, Zhang D, Zhu H, Zhu J, Weng S, Dong L, Liu T, Hu Y, Shen X. Berberine treatment increases Akkermansia in the gut and improves high-fat diet-induced atherosclerosis in Apoe-/- mice. Atherosclerosis. 2018 Jan;268:117-126. doi: 10.1016/j.atherosclerosis.2017.11.023. Epub 2017 Nov 24. PMID: 29202334.

[40] Liu Z, Qiao Q, Sun Y, Chen Y, Ren B, Liu X. Sesamol ameliorates diet-induced obesity in C57BL/6J mice and suppresses adipogenesis in 3T3-L1 cells via regulating mitochondria-lipid metabolism. Mol Nutr Food Res. 2017 Aug;61(8). doi: 10.1002/mnfr.201600717. Epub 2017 Feb 7. PMID: 28012248.

[41] Mehlem, A., Hagberg, C., Muhl, L. et al. Imaging of neutral lipids by oil red O for analyzing the metabolic status in health and disease. Nat Protoc 8, 1149–1154 (2013). https://doi.org/10.1038/nprot.2013.055